Available online at www.sciencedirect.com

ScienceDirect

IFAC PapersOnline CONFERENCE PAPER ARCHIVE

IFAC PapersOnLine 53-2 (2020) 14509–14516

On Collision Risk Assessment for Autonomous Ships Using Scenario-Based MPC

Tengesdal, Trym * **Brekke, Edmund F.** * **Johansen, Tor A.** *

* *Center for Autonomous Marine Operations and Systems (AMOS). Department of Engineering Cybernetics, NTNU - Norwegian University of Science and Technology, O.S. Bragstads plass 2D N-7491, Trondheim, Norway (e-mail: {trym.tengesdal, edmund.brekke, tor.arne.johansen}@ntnu.no)*

Abstract: Collision Avoidance (COLAV) for autonomous ships is challenging since it relies on track estimates of nearby obstacles which are inherently uncertain in both state and intent. This uncertainty must be accounted for in the COLAV system in order to ensure both safe and efficient operation of the vessel in accordance with the traffic rules. Here, a COLAV system built on the Scenario-based Model Predictive Control (SB-MPC) with dynamic probabilistic risk treatment is presented. The system estimates the probability of collision with all nearby obstacles using a combination of Monte Carlo simulation (MCS) and a Kalman Filter (KF), taking the uncertainty in both position and velocity into account. A probabilistic collision cost is then used in the MPC to penalize risk-taking maneuvers. Simulation results show that the proposed method may provide increased robustness due to increased situational awareness, while also being able to efficiently follow the nominal path and adhere to the traffic rules.

Keywords: COLREGS, Collision avoidance, Autonomous ships, Model Predictive Control, Probabilistic risk assessment, Kalman Filter, Monte Carlo simulation

1. INTRODUCTION

A big challenge in the maritime transport sector is the safety aspect. Significant consequences in the form of human casualties, environmental damage and destruction of properties are caused by vehicle collisions every year. Ship collisions and groundings caused 5573 casualty events in the period from 2011 to 2017, according to the European Maritime Safety Agency (EMSA, 2018). Humans are reported to be the main cause in excess of 75 % of the time (Macrae, 2009; Chauvin, 2011; Levander, 2017). The emergence of autonomous ships may therefore increase safety, by eliminating the human factor.

Autonomous ships utilize a tracking system to receive information about nearby obstacles, which may include commercial and recreational vessels. The performance of the COLAV system is therefore limited to the quality of the track estimates, which fuse uncertain obstacle kinematics and sensor data. Other factors such as the intent and behavior of the obstacles to the ship maneuvers will heavily affect this uncertainty, and make the situation challenging. The quality of information is thus important for deliberative COLAV algorithms, which are supposed to take proactive actions in due time before the potential collision hazard occurs.

Furthermore, the ship should comply with the International Regulations for Avoiding Collision at Sea (COLREGS) (IMO, 1972), which classify different collision situations, the vessels involved and the rules to follow in the situations. Here, rules 8, 13-17 are the most relevant, and defines the required vessel classifications and actions in general, and the correct behavior in overtaking, head-on and crossing situations. These situations, which are described in rules 13-15, are graphically illustrated in Figure 1. Rule 8 states that actions to avoid collision should be clear and taken in ample time. Rule 16 and 17 describe the actions to be performed by the give-way vessel and stand-on vessel, which involve the requirements to take an early and clear action, and maintaining its current course and speed if possible, respectively. However, for situations involving multiple vessels, it may be necessary to violate COLREGS in order to avoid collision.

There are many existing COLAV algorithms which have COLREGS compliance at varying degree. However, only a few of these are performing probabilistic risk assessment in collision situations considering uncertainties present, as this has mostly been ignored for such systems (Huang et al., 2020). The COLAV problem will involve considering uncertainties present in the current situation, taking these into account, and then choosing the risk minimizing action. Deterministic approaches will therefore have limitations for efficient and robust COLAV systems. For a general treatment of different collision risk measures, see for instance Goerlandt and Montewka (2015) and Chen et al. (2019). Relevant maritime COLAV algorithms which incorporate some form of probabilistic risk measure are summarized below.

10.1016/j.ifacol.2020.12.1454

In Shah et al. (2016), an A* search method is applied to collision free path planning which penalizes high collision risk, COLREGS breaches and path deviation. The collision risk is estimated by calculating collision probabilities using sampling based techniques, considering the positional uncertainty. A* search is also used in Blaich et al. (2015), to plan a collision free path through an occupancy grid. Here, occupancy probabilities for obstacles in two-dimensional space are calculated using a numerical approximation, considering their kinematic uncertainty. The search then tries to find a path which minimizes the cost due to non-zero occupancy probabilities, and the Euclidean distance to the goal. COLREGS is not considered here.

In Park et al. (2019), MCS is used to estimate the collision probability beween the own-ship and an obstacle, both with time varying uncertainty. This is done by first forming a Probability Density Function (PDF) at the tracked obstacle position, with a covariance that is the sum of the estimated vessel position covariances. The ratio of samples drawn from this PDF that are inside a Collision Risk Zone (CRZ), to the total number of samples, is used as a collision probability estimate. The collision probability estimate is then used to decide on replanning collision free waypoints for the ship to follow, which also adhere to the COLREGS.

Rajendran et al. (2018) plans a collision free path using Theta* search, based on the current locally estimated sea state, nearby static and dynamic obstacles, and own-ship motion uncertainty. MCS is used to sample dynamic obstacle positions and velocities based on their perception uncertainty, and used together with a precomputed State Transition Table (STT) to index an estimated Mean Time Between Failure (MTBF) for the USV, which is then used to estimate the probability of failure in reaching a motion goal due to collision and local environmental disturbances. This failure probability is then penalized in the search cost function, together with path execution time and COLREGS breaches.

Maneuvering intentions of an obstacle are estimated using a KF in Cho and Kim (2017). The intentions are used to calculate the collision probability with obstacles by considering reachable sets. A COLAV system then makes evasive maneuvers when the collision probability exceeds a certain threshold, with no COLREGS consideration.

The proposed method is a probabilistic version of the Scenario-based Model Predictive Control by Johansen et al. (2016), i.e. Probabilistic SB-MPC (PSB-MPC). Here, the probability of collision with nearby obstacles is estimated, and used to minimize the collision risk on the prediction horizon. A novel contribution is how the collision probabilities are estimated through the use of MCS combined with a KF for the attenuation of statistical noise resulting from few MCS samples. The uncertainty in both position and velocity for the obstacles are considered, as obtained from a tracking system based on the KF. This gives increased situational awareness for the autonomous ship, as the kinematic uncertainty in both position and velocity is an information source not being used in most COLAV systems.

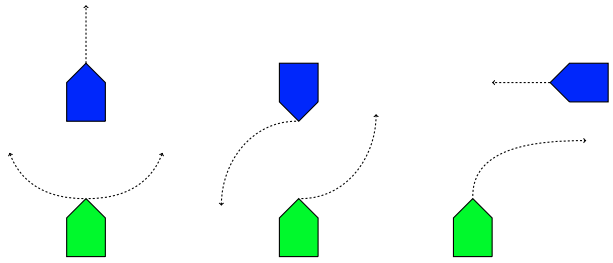

Fig. 1. COLREGS situations. From left to right: Overtaking, head-on and crossing situations. The arrows indicate the correct behavior in each situation.

This article is organized as follows: In Section 2, the own-ship model used for guidance, control and prediction, and the obstacle model used in the tracking system and MPC predictions, are presented. The original SB-MPC is reviewed in Section 3. The collision probability framework used here is introduced in Sections 4-5, whereas the PSB-MPC is introduced in Section 6. Results comparing the PSB-MPC against the original SB-MPC are then given in Section 7, before conclusions are summarized in Section 8.

2. MODELS

2.1 Ship Dynamics

A model with 3 degrees of freedom (DOF) is used to describe the horizontal motion of the own-ship in surge, sway and yaw (Fossen, 2011). The vessel position in the North-East-Down (NED) coordinate system is given by $\boldsymbol{\eta} = [\, x \;\; y \;\; \psi \,]^T$. The variables x, y and ψ are the own-ship north and east coordinates and the heading, respectively. The ship velocity in the BODY-fixed coordinate system is given as $\boldsymbol{\nu} = [\, u \;\; v \;\; r \,]^T$. Here, u and v are the surge and sway velocity, respectively, while r is the yaw rate. The vector $\boldsymbol{\tau} = [\, X \;\; Y \;\; N \,]^T$ describes the generalized forces and moments affecting the ship in surge, sway and yaw. The equations of motion for the own-ship can then be represented in vectorial form as

$$\dot{\boldsymbol{\eta}} = \boldsymbol{R}(\psi)\boldsymbol{\nu} \tag{1}$$

$$\boldsymbol{M}\dot{\boldsymbol{\nu}} + \boldsymbol{C}(\boldsymbol{\nu})\boldsymbol{\nu} + \boldsymbol{D}(\boldsymbol{\nu})\boldsymbol{\nu} = \boldsymbol{\tau} + \boldsymbol{w} \tag{2}$$

where $\boldsymbol{R}(\cdot)$ is the rotation matrix from the NED frame $\{n\}$ to the BODY frame $\{b\}$, $\boldsymbol{M}$ is the inertia matrix, $\boldsymbol{C}(\cdot)$ the coriolis and centripetal matrix and $\boldsymbol{D}(\cdot)$ the nonlinear damping matrix. The environmental disturbances are not considered here since they are compensated for in the autopilot, thus $\boldsymbol{w} = 0$. The position and velocity of the own-ship is assumed to be accurately measured, and thus its uncertainty in position and velocity is neglected. The own-ship is steered using Line of Sight (LOS) guidance (Fossen, 2011), with a feedback linearizing controller used for surge, and a PD-controller for the heading. See Tengesdal (2019) for details.

2.2 Obstacle Dynamics

The Constant Velocity Model (CVM) is common for predicting the trajectories of nearby obstacles (Bar-Shalom and Li, 1995), and the general stochastic form is in discrete time for obstacle $i = 1, 2, \ldots n_o$ given as

$$\boldsymbol{x}_{k+1}^i = \boldsymbol{F}\boldsymbol{x}_k^i + \boldsymbol{v}_k^i \tag{3}$$

$$\boldsymbol{z}_k^i = \boldsymbol{H}\boldsymbol{x}_k^i + \boldsymbol{w}_k^i \tag{4}$$

where $\boldsymbol{x}^i = [\, x^i \;\; y^i \;\; V_x^i \;\; V_y^i \,]^T$ is the state vector consisting of the 2D position and velocity, and where $\boldsymbol{F}$ and $\boldsymbol{H}$ are the transition and measurement matrix, respectively. Index $k = 1, 2, \ldots N$ denotes the time step. The vectors $\boldsymbol{v}_k^i$ and $\boldsymbol{w}_k^i$ are the process and measurement noise at discrete time instant t_k, respctively. The vector $\boldsymbol{z}_k^i$ contains the noise corrupted position measurement at time t_k for instance obtained through a radar system or Automatic Identification System (AIS) data. The transition matrix $\boldsymbol{F}$ and measurement matrix $\boldsymbol{H}$ are given as

$$\boldsymbol{F} = \begin{bmatrix} 1 & 0 & T_s & 0 \\ 0 & 1 & 0 & T_s \\ 0 & 0 & 1 & 0 \\ 0 & 0 & 0 & 1 \end{bmatrix} \tag{5}$$

$$\boldsymbol{H} = \begin{bmatrix} 1 & 0 & 0 & 0 \\ 0 & 1 & 0 & 0 \end{bmatrix} \tag{6}$$

where $T_s = t_{k+1} - t_k$ is the sampling interval for the linear model, which could be time varying. The process noise and measurement noise are assumed to be zero mean, white, mutually independent and Gaussian with known covariance matrices $\boldsymbol{Q}$ and $\boldsymbol{R}$, respectively. The process noise covariance is given as

$$\boldsymbol{Q} = \sigma_a^2 \begin{bmatrix} \frac{T_s^3}{3} & 0 & \frac{T_s^2}{2} & 0 \\ 0 & \frac{T_s^3}{3} & 0 & \frac{T_s^2}{2} \\ \frac{T_s^2}{2} & 0 & T_s & 0 \\ 0 & \frac{T_s^2}{2} & 0 & T_s \end{bmatrix} \tag{7}$$

where the process noise strength σ_a is chosen based on the expected maneuverability of the vessel (Wilthil et al., 2017). The CVM is used with the KF for tracking the obstacles, which results in multivariate Gaussian PDFs $p^i(\boldsymbol{x}, t_k) = \mathcal{N}(\boldsymbol{x}; \hat{\boldsymbol{x}}_k^i, \boldsymbol{\Sigma}_k^i)$, where $\hat{\boldsymbol{x}}_k^i$ and $\boldsymbol{\Sigma}_k^i$ are the obstacle track estimate and associated covariance, respectively. A deterministic CVM with the full state vector available, obtained by omitting the noise terms, is used in the MPC predictions. Note that the CVM assumption has limitations in scenarios where maneuvers are expected, as for instance in ship encounters.

3. ORIGINAL SCENARIO-BASED MODEL PREDICTIVE CONTROL

The SB-MPC (Johansen et al., 2016) is a scenario-based optimization method for COLAV, which solves the optimization problem

$$l^*(t_0) = \arg\min_l \mathcal{H}^l(t_0) \tag{8}$$

The index l represents a candidate control behavior, which consist of a modification tuple (χ_m^l, u_m^l) to the current guidance references χ_d and u_d in course and forward speed, respectively. A finite set of control behaviors is typically considered, for which the cost function

$$\begin{aligned} \mathcal{H}^l(t_0) = \max_i \max_{t \in D(t_0)} \left(\mathcal{C}_i^l(t) \mathcal{R}_i^l(t) + \kappa_i \mu_i^l(t) \right) \\ + f(\chi_m^l, \chi_{m,last}, u_m^l, u_{m,last}) + g(\cdot) \end{aligned} \tag{9}$$

is evaluated. Here, t_0 is the current time and $D(t_0)$ is the set of time steps in the prediction horizon T. The variables $\mathcal{C}_i^l(t)$ and $\mathcal{R}_i^l(t)$ are the collision cost and ad hoc collision risk associated with obstacle i at the prediction time t, respectively. The term $\kappa_i \mu_i^l(t)$ quantify the COLREGS violation, where κ_i is a tuning parameter and $\mu_i^l(t) \in \{0, 1\}$ a binary indicator for breaching COLREGS. Finally, $f(\cdot)$ and $g(\cdot)$ are the control reference deviation and grounding costs, respectively. No grounding cost is used here, such that $g(\cdot) = 0$. See the original work (Johansen et al., 2016) for more information about the cost terms. The control reference deviation cost $f(\cdot)$ is here modified to

$$\begin{aligned} f(\cdot) = K_u(1 - u_m^l) + K_\chi(\chi_m^l) \\ + \Delta_u(u_m^l, u_{m,last}) + \Delta_\chi(\chi_m^l, \chi_{m,last}) \end{aligned} \tag{10}$$

where

$$K_\chi(\chi) = \begin{cases} K_{\chi,\text{port}} \chi^2, & \text{if } \chi < 0. \\ K_{\chi,\text{starboard}} \chi^2, & \text{otherwise,} \end{cases} \tag{11}$$

$$\Delta_u(u_1, u_2) = K_{\Delta u} |u_1 - u_2|, \tag{12}$$

$$\Delta_\chi(\chi_1, \chi_2) = \begin{cases} K_{\Delta_{\chi,\text{port}}} (\chi_1 - \chi_2)^2, & \text{if } \chi_1 < 0. \\ K_{\Delta_{\chi,\text{starboard}}} (\chi_1 - \chi_2)^2, & \text{otherwise.} \end{cases} \tag{13}$$

The tuning parameters K_u, $K_{\chi,-}$, $K_{\Delta u}$ and $K_{\Delta_{\chi,-}}$ determine the penalization on the course and surge modifications, where $-$ is a placeholder for either port or starboard. This modification of $f(\cdot)$ is done in order to penalize course changes to port more than starboard, to make it easier for the algorithm to follow COLREGS. The optimal control behavior then modifies the course and forward speed references χ_d and u_d from the guidance system through $\chi_c = \chi_m^{l^*} + \chi_d$ and $u_c = u_m^{l^*} \cdot u_d$. The objective of the present article is to replace the ad hoc collision cost term $\mathcal{C}_i^l(t)\mathcal{R}_i^l(t)$ with a probabilistic collision cost.

4. COLLISION PROBABILITY DEFINITION

Probabilities are always relative to the domain of events considered, and a clear definition is therefore needed to avoid amibiquity and confusion. Here, the following events are used to define the collision probability between the own-ship and an obstacle.

$$\begin{aligned} &\mathcal{A}_k^i = \textit{A collision occurs between obstacle } i \textit{ and the} \\ &\quad \textit{own-ship at some time } t_c \geq t_k. \end{aligned} \tag{14}$$

$\mathcal{B}_k^i$ = *A collision between obstacle i and the own-ship does not occur at any time $t_c \geq t_k$.* (15)

which are mutually exclusive. Collision is the breach of the safety zone, which is defined as a circular region with radius d_{safe} around the own-ship. The probability of collision with obstacle i at time t_k then becomes

$$\mathbb{P}_{c,k}^i = P\{\mathcal{A}_k^i\} = 1 - P\{\mathcal{B}_k^i\} \tag{16}$$

Note that this definition of collision probability is predictive, as it allows for the collision to happen at any time in the future. The collision probability $\mathbb{P}_{c,k}^i$ is found by integrating the obstacle tracked state PDF $p^i(\boldsymbol{x}, t_k)$:

$$\mathbb{P}_{c,k}^i = \int_{\mathcal{S}} p^i(\boldsymbol{x}; t_k) d\boldsymbol{x} \tag{17}$$

where $\mathcal{S} \subset \mathbb{R}^4$ is a region which include all straight line trajectories which make the obstacle cross and recide in the own-ship safety zone at the Closest Point of Approach (CPA) (Tengesdal, 2019). This makes the formulation of a compact $\mathcal{S}$ difficult, due to time being an implicit constraint. More specifically, the integration limits on the obstacle velocities depend on both the starting position (x_k^i, y_k^i) of the obstacle, which is uncertain, and the time interval for which the given trajectory starting at (x_k^i, y_k^i) gives an obstacle position inside the own-ship safety zone at CPA.

An illustration of the issue is given in Figure 2, where a sample trajectory based on the obstacle uncertainty in position and velocity is shown. The own-ship is shown in blue at the current time following a straight line trajectory, and also at the CPA in dashed blue with the safety zone of radius d_{safe} enclosing it. The obstacle is shown in green at the current time with its 3σ position probability ellipse. If the time to CPA gives an obstacle position on the indicated red part of the trajectory, the trajectory is in $\mathcal{S}$ and may result in a collision.

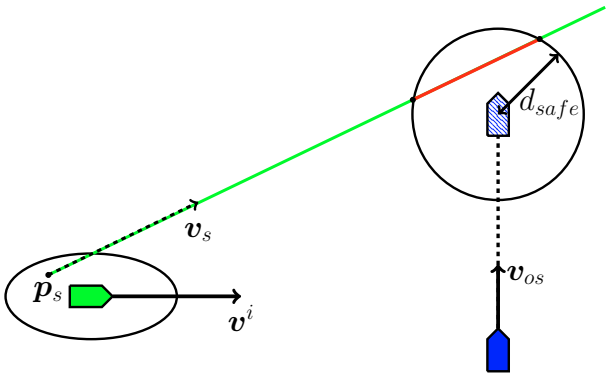

Fig. 2. Illustration of the problem of determining if an obstacle trajectory is in $\mathcal{S}$. The sampled obstacle trajectory is given by the sampled starting position $\boldsymbol{p}_s$ and velocity $\boldsymbol{v}_s$. The expected obstacle velocity $\boldsymbol{v}^i$ and own-ship velocity $\boldsymbol{v}_{os}$ are also indicated.

5. COLLISION PROBABILITY ESTIMATION

The calculated collision probability between the own-ship and obstacle i is here filtered recursively using a KF (Kalman, 1960). Probabilities calculated through MCS to approximate the integral (17) are used as measurements. The KF is used to attenuate the statistical noise inherent in the MCS with a finite number of samples, and to make use of knowledge about the collision probability from the previous time step. The simple model used in the KF is

$$\mathbb{P}_{c,k+1}^i = \mathbb{P}_{c,k}^i + \bar{v}_k^i \tag{18a}$$
$$y_k^i = \mathbb{P}_{c,k}^i + \bar{w}_k^i \tag{18b}$$

where y is the measurement, $\bar{v} \sim \mathcal{N}(\bar{v}; 0, q_P)$ and $\bar{w} \sim \mathcal{N}(\bar{w}; 0, r_P)$ are the process and measurement noise, respectively. The collision probability measurement y_k^i is obtained through MCS as

$$y_k^i = \frac{1}{N_{MC}} \sum_{s=1}^{N_{MC}} I\{\boldsymbol{x}_s \in \mathcal{S}\} p^i(\boldsymbol{x}_s, t_k) \tag{19}$$

where N_{MC} is the number of samples drawn from the obstacle tracked state PDF. This is done by sampling from a standard normal distribution, followed by a transformation through the obstacle state estimate $\hat{\boldsymbol{x}}_k^i$ and Cholesky factorization of the obstacle state covariance $\boldsymbol{\Sigma}_k^i$. The indicator variable $I\{\boldsymbol{x}_s \in \mathcal{S}\} \in \{0, 1\}$ determines if the straight line trajectory sample parameterized by $\boldsymbol{x}_s$ makes the obstacle cross and recide inside the own-ship safety zone at the CPA, assuming that the own-ship also follows a straight line trajectory at time t_k. These assumptions are made in order to have a tractable approach of calculating the collision probability.

In general, an integral estimate obtained through MCS is consistent by the law of large numbers, when the underlying probability model is accurate (Evans and Rosenthal, 2009). In this case, the consistency of the collision probability estimate produced by the MCS and KF are conditioned on the validity of the assumptions of obstacles being modelled as CVMs with Gaussian distributed states, the validity of the model (18), and the own-ship being assumed to also follow a straight line trajectory at the time of probability calculation. Thus, it is typically a conservative estimate, as factors such as the own-ship and obstacles' intention of avoiding collision and adhering to COLREGS are not accounted for. The estimate will anyhow be used here as an indication of the collision risk. An increased situational awareness by the autonomous ship will be gained regardless, due to the tracking uncertainty being used to have a probabilistic risk picture.

Simulation results for a simple scenario with one obstacle are shown in Figure 3. Here, the own-ship is stationary at coordinates $(x, y) = (100, 0)$, whereas an obstacle starting at $(55, -55)$ with assumed known expected position is travelling east with speed 4 m/s. The safety zone is indicated as the red circle. The obstacle is shown at CPA, directly south the own-ship at time $t = 13.75$ s, and also at the end of the simulation. A number of $N_{MC} = 100$ samples are used. The noise covariances are tuned to be

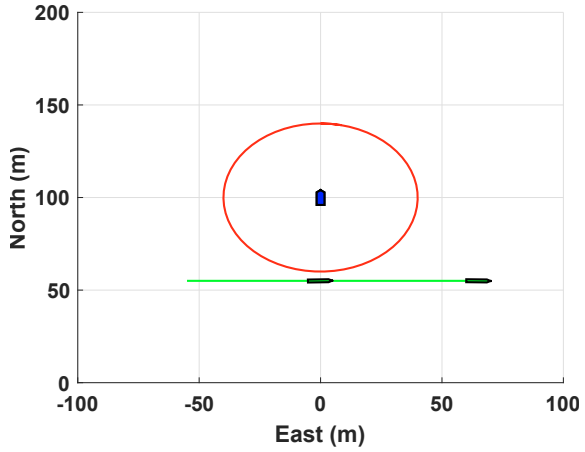

(a) North east plot of the own-ship (blue) and obstacle (green).

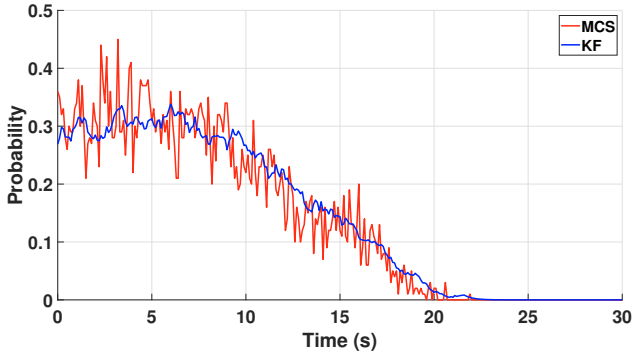

(b) Collision probability between the own-ship and obstacle estimated with a KF and the "measurements" obtained through MCS.

Fig. 3. Test scenario

$q_P = 0.00005$ and $r_P = 0.001$, based on trial and error and Normalized Innovation Error (NIS) considerations (Bar-Shalom and Li, 2001). The filter was initialized with prior probability and variance of 0 and 0.3, respectively. This was partially based on an initial guess, and the assumption that the own-ship starts relatively far from nearby obstacles. The obstacle tracked state has a constant covariance matrix of $\mathbf{\Sigma} = \text{diag}([25\ 25\ 4\ 4])$, which causes the collision probability to have a maximum right above 0.3, and decreasing as it passes the own-ship, due to the number of possible straight line trajectories which can cross the safety zone decreases.

Thus, from the results, the advantage in using MCS and KF for collision probability estimation is apparent in the reduction of statistical noise at lower computational cost than pure MCS, as fewer samples are needed in the MCS calculations.

6. THE PROBABILISTIC SCENARIO-BASED MODEL PREDICTIVE CONTROL

A Probabilistic variant of the SB-MPC modifies the cost function (9) to

$$\mathcal{H}^l(t_0) = \max_i \left(\sum_{t \in D(t_0)} \mathcal{C}_i^l(t) \hat{\mathbb{P}}_c^{l,i}(t) e^{-\frac{(t + t_{cpa}^l(t) - t_0)}{T_c}} + \max_{t \in D(t_0)} \kappa_i \mu_i^l(t) \right) + f(\cdot) + g(\cdot) \tag{20}$$

involving the accumulated probabilistic collision cost over the horizon, exponentially discounted by the time until the potential collision. Thus, the ad hoc risk term $\mathcal{R}_i^l$ is replaced by the collision probability estimate $\hat{\mathbb{P}}_c^{l,i}$. The discounting type was chosen mainly due to its simplicity and common use for devaluating events or data, as for instance in the recursive least squares method (Ioannou and Sun, 2012). The time constant T_c is a tuning parameter. The variable t_{cpa}^l indicates the time until the CPA between the own-ship and obstacle i occurs, calculated at the time t using the corresponding predicted states. As the collision probability is predictive, the time until CPA is added to weight the collision cost by the time of occurrance. Note that this is under the assumption of straight line trajectories at the time of calculation. Moreover, because the collision probabilities are summed, it is assumed that they are independent from one time step to another. This is conservative, as there will be dependencies due to obstacle dynamics and the fact that at maximum one collision between the own-ship and an obstacle can occur in the horizon.

A reasonable alternative to this MPC formulation would be to use a collision risk constraint instead, to retain the risk to a certain limit. However, due to the consistency issues mentioned in the previous section, the constraint limit would be ad hoc. Further, as the collision probability calculations are done in the open loop MPC predictions, with no future feedback accounted for, the limit should not be set too low. Moreover, issues with constraint infeasibility would need to be solved with slack variables to allow practical use.

The advantage of penalizing the collision cost as in the original SB-MPC, is the guarantee of a feasible solution and the intution of balancing the cost terms. With this approach one is able to choose the maneuver with minimum probabilistic collision cost, which would not be possible in a risk constrained PSB-MPC, as maneuvers are only deemed feasible or not. However, in situations with high collision risk for all control behaviors, the optimally chosen maneuver may still be infeasible in practice and possibly lead to collision, which would require extra handling with this MPC formulation.

7. RESULTS

The PSB-MPC and SB-MPC were tested in a head-on scenario, and a congested traffic scenario with multiple obstacles. A sampling interval of $T_s = 0.1\,\text{s}$ was used for the obstacle motion and as the step time in Euler's method to simulate the own-ship motion. A sample time of $T_{s,MPC} = 0.5\,\text{s}$ was used for the MPC. The own-ship was in each scenario planned to follow the straight line going north, with forward speed $u_d = 9\,\text{m/s}$, starting in the origin. The obstacles were randomly initialized inside

a grid of 1000m × 800m, with obstacle velocities varying from 2 m/s to $v^i_{max} = 9$ m/s. The process noise parameter σ_a was uniformly randomly generated between 0 m/s^2 and 0.03 m/s^2 for each obstacle. This simulates scenarios with vessels of lengths around 30 m, driving around cruising speed and below. A measurement covariance of $\boldsymbol{R} = \text{diag}([25\ 25])\text{m}^2$ was used to generate obstacle position measurements at 0.4 Hz, with values based on the results using a radar-based tracker in (Wilthil et al., 2017).

Kalman Filters were used to track each obstacle, with the track estimates fed into the PSB-MPC and SB-MPC. The corresponding covariance estimates were used in the collision probability calculation of the PSB-MPC for the entire time horizon. Thus, the tracked state covariance was not propagated using a deterministic CVM in the MPC predictions, but kept constant. This simplification makes the collision probability estimate less conservative, as the covariance would increase when propagated in time. As nearby obstacles will in reality react to the own-ship maneuvers, and measurements of their positions will be used to reduce the uncertainty, this was deemed reasonable. Further, single-point track initiation was used for the obstacle estimates based on the results in (Mallick and Scala, 2008), where the obstacle initial position and velocity are set to the first measurement and zero, respectively. The a priori obstacle state covariance is set using the KF measurement covariance matrix and maximum velocity U^i_{max}, where it is here assumed that the maximum speed is known a priori, and identical for all obstacles.

To illustrate the importance of considering kinematic uncertainty in a COLAV system, the KF in the tracking system was tuned conservatively in both scenarios with a measurement covariance matrix 25 times larger than the actual covariance $\boldsymbol{R}$, and process noise parameter $\sigma_a = 0.5$ m/s^2 for all obstacles. This can be the case when measurements from a radar device becomes unreliable due to extreme weather conditions, and where one in addition wants to account for fast obstacle maneuvers by having an increased process noise. This combined with the chosen track initialization, will cause more uncertain obstacle course estimates, which has been shown to cause problems in deterministic reactive COLAV systems (Eriksen et al., 2018).

The collision probability filter was again initialized with prior probability and variance of 0 and 0.3, respectively. The parameters used for each COLAV method are summarized in Table 1, and are partially based on (Hagen, 2017) and trial and error. The COLAV methods are run every fifth second in the simulations, with 39 control behaviors with one planned evasive maneuver on the prediction horizon.

Results comparing the original SB-MPC and the PSB-MPC are shown in Figure 4 and 5. In each Figure, the first part shows a north east plot for the own-ship with the original SB-MPC (blue boat with black trajectory) and the PSB-MPC (red boat with dashed black trajectory), with the safety zone of radius d_{safe} enclosing them. Also, the obstacles are shown as green boats, with numbered trajectories of different colors. The second part shows the distance from the own-ship to each obstacle, for both COLAV versions, with the safe distance also indicated in red. The obstacle and own-ship sizes are enlarged for visualization purposes. The scenario in Figure 4 also include a track plot.

The scenario in Figure 4 shows that the PSB-MPC is more risk averse than the original SB-MPC by taking a COLREGS compliant maneuver with larger safety margins. In contrast, the SB-MPC trusts the obstacle track estimate blindly, which causes a small safety zone violation while performing the COLREGS compliant maneuver. This is because the SB-MPC believes the obstacle is travelling south with a negative east speed for the first 37 seconds. This is caused by the high obstacle track uncertainty coming from a conservatively tuned KF and the Single-Point track initialization, which causes a velocity variance surpassing 20(m/s)^2 in each direction initially.

Figure 5 shows that the PSB-MPC is capable of making safe maneuvers in more complex scenarios. Here, the original SB-MPC violates COLREGS slightly and makes a poor decision to turn port, due to its overconfidence in the obstacle track estimates. This is because obstacles are initialized to zero speed, which makes a port maneuver optimal in the SB-MPC as this gives the minimum ad hoc collision cost. The PSB-MPC again accounts for the estimated uncertainty and decide on a starboard maneuver, due to its minimum probabilistic collision cost.

8. CONCLUSION

The PSB-MPC attempts to take dynamic collision probabilities into account, which considers uncertainty in both position and velocity, and is able to take safe decisions in complex scenarios due to increased situational awareness. The probabilistic collision cost gives larger safety margins, but this is conditioned on the quality of the track estimates and collision probability estimates. Simulation results show that its performance with regards to path following is also on par with the original SB-MPC. Note that the PSB-MPC formulated here is preliminary, and aims to illustrate the benefits of introducing probabilistic risk assessment in a COLAV system.

Moreover, as the method for calculating collision probabilities is simplistic, based on straight line trajectory assumptions, and relatively slow, work is needed in order to make the calculations more efficient and also more con-

Table 1. Parameters for the COLAV methods.

	SB-MPC	**PSB-MPC**
Parameter	**Value**	**Value**
T	200 s	200 s
$T_{s,MPC}$	0.5 s	0.5 s
d_{safe}	40 m	40 m
κ_i	10.0	10.0
K_{u_m}	9.0	9.0
$K_{\Delta_{u_m}}$	8.0	8.0
$K_{\chi,\text{port}}$	1.8	1.8
$K_{\chi,\text{starboard}}$	1.5	1.5
$K_{\Delta_{\chi,\text{port}}}$	1.2	1.2
$K_{\Delta_{\chi,\text{starboard}}}$	0.9	0.9
T_c	-	6 s
N_{MC}	-	100
q_P	-	0.00005
r_P	-	0.001

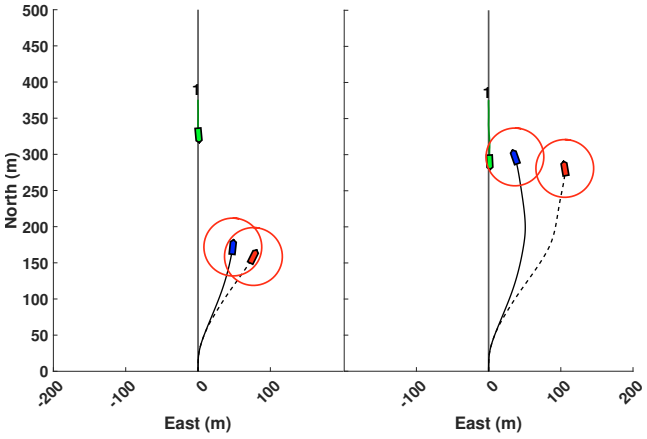

(a) North east plot of the own-ship and obstacle at two time instants.

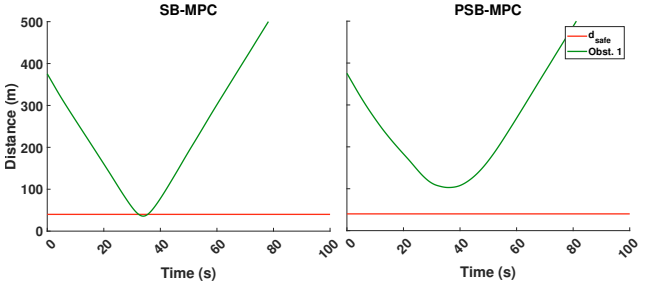

(b) Distance from the own-ship to the obstacle, for both versions of the SB-MPC.

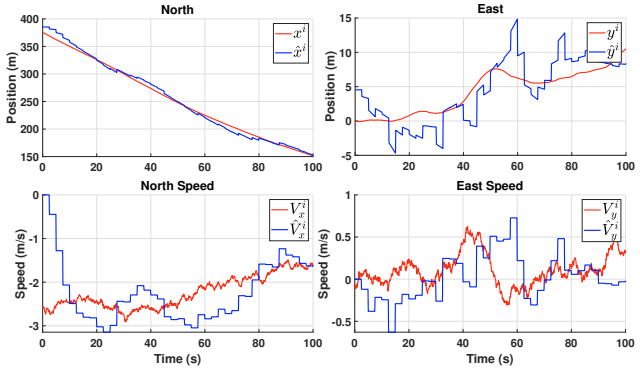

(c) True obstacle state (red) versus the tracked state (blue).

Fig. 4. Head-on scenario with 1 obstacle.

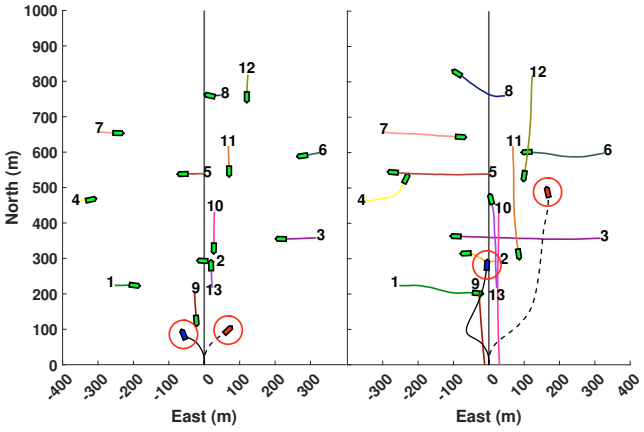

(a) North east plot of the own-ship and obstacles at two time instants.

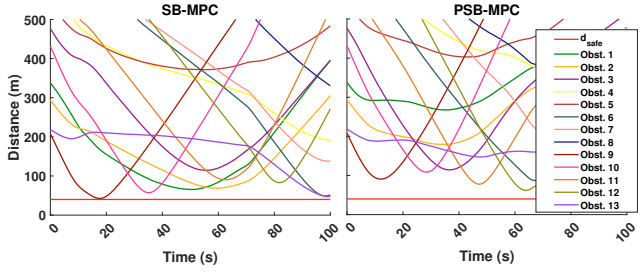

(b) Distance from the own-ship to each obstacle, for both versions of the SB-MPC.

Fig. 5. Congested traffic scenario with 13 obstacles.

sistent and realistic by considering obstacle manoeuvres and probabilistic COLREGS compliance.

ACKNOWLEDGEMENTS

This work was supported by the Research Council of Norway through the Centers of Excellence funding scheme, project number 223254, Centre for Autonomous Marine Operations and Systems.

REFERENCES

Bar-Shalom, Y. and Li, X.R. (1995). *Multitarget-multisensor tracking: principles and techniques*, volume 19. YBs Storrs, CT.

Bar-Shalom, Y. and Li, X.R. (2001). *Estimation with Applications to Tracking and Navigation: Theory, Algorithms and Software*. John Wiley & Sons, Inc., New York, NY, USA.

Blaich, M., Köhler, S., Reuter, J., and Hahn, A. (2015). Probabilistic collision avoidance for vessels. *IFAC-PapersOnLine*, 48(16), 69–74.

Chauvin, C. (2011). Human factors and maritime safety. *Journal of Navigation*, 64, 625 – 632.

Chen, P., Huang, Y., Mou, J., and van Gelder, P. (2019). Probabilistic risk analysis for ship-ship collision: State-of-the-art. *Safety Science*, 117, 108–122. URL `https://www.scopus.com/inward/record.uri?eid=2-s2.0-85064275718&doi=10.1016%2fj.ssci.2019.04.014&partnerID=40&md5=f14a25f3704e4b3167029568dd76e8a0`.

Cho, Y. and Kim, J. (2017). Collision probability assessment between surface ships considering maneuver intentions. In *Proc. OCEANS 2017 - Aberdeen*, 1–5. doi:10.1109/OCEANSE.2017.8084791.

EMSA (2018). The european maritime safety agency: Annual overview of marine casualties and incidents. URL `http://www.emsa.europa.eu/emsa-documents/latest/item/3406-annual-overview-of-marine-casualties-and-incidents-2018.html`.

Eriksen, B.H., Wilthil, E.F., Flåten, A.L., Brekke, E.F., and Breivik, M. (2018). Radar-based maritime collision avoidance using dynamic window. In *2018 IEEE Aerospace Conference*, 1–9.

Evans, M. and Rosenthal, J. (2009). *Probability and Statistics: The Science of Uncertainty*. W. H. Freeman.

Fossen, T.I. (2011). *Handbook of marine craft hydrodynamics and motion control*. John Wiley & Sons.

Goerlandt, F. and Montewka, J. (2015). Maritime transportation risk analysis: review and analysis in light of some foundational issues. *Reliability Engineering & System Safety*, 138, 115–134.

Hagen, I.B. (2017). *Collision Avoidance for ASVs Using Model Predictive Control*. Master's thesis, NTNU.

Huang, Y., Chen, L., Chen, P., Negenborn, R.R., and van Gelder, P. (2020). Ship collision avoidance methods: State-of-the-art. *Safety Science*, 121, 451 – 473. URL `http://www.sciencedirect.com/science/article/pii/S0925753519306356`. Unpublished.

IMO (1972). COLREGS - International Regulations for Preventing Collisions at Sea. *Convention on the International Regulations for Preventing Collisions at Sea, 1972*.

Ioannou, P. and Sun, J. (2012). *Robust Adaptive Control*. Dover Publications Inc.

Johansen, T.A., Perez, T., and Cristofaro, A. (2016). Ship collision avoidance and COLREGS compliance using simulation-based control behavior selection with predictive hazard assessment. *IEEE Transactions on Intelligent Transportation Systems*, 17(12), 3407–3422.

Kalman, R.E. (1960). A new approach to linear filtering and prediction problems. *Journal of basic Engineering*, 82(1), 35–45.

Levander, O. (2017). Autonomous ships on the high seas. *IEEE Spectrum*, 54(2), 26–31.

Macrae, C. (2009). Human factors at sea: common patterns of error in groundings and collisions. *Maritime Policy & Management*, 36(1), 21–38.

Mallick, M. and Scala, B.L. (2008). Comparison of single-point and two-point difference track initiation algorithms using position measurements. *Acta Automatica Sinica*, 34(3), 258 – 265. URL `http://www.sciencedirect.com/science/article/pii/S1874102908600117`.

Park, J., Choi, J., and Choi, H. (2019). COLREGS-compliant path planning considering time-varying trajectory uncertainty of autonomous surface vehicle. *Electronics Letters*, 55(4), 222–224.

Rajendran, P., Moscicki, T., Wampler, J., Shah, B.C., von Ellenrieder, K., and Gupta, S.K. (2018). Wave-aware trajectory planning for unmanned surface vehicles operating in congested environments. In *2018 IEEE International Symposium on Safety, Security, and Rescue Robotics (SSRR)*, 1–7.

Shah, B.C., Švec, P., Bertaska, I.R., Sinisterra, A.J., Klinger, W., von Ellenrieder, K., Dhanak, M., and Gupta, S.K. (2016). Resolution-adaptive risk-aware trajectory planning for surface vehicles operating in congested civilian traffic. *Autonomous Robots*, 40(7), 1139–1163.

Tengesdal, T. (2019). *Uncertainty Management in an SB-MPC for Collision Avoidance*. Master's thesis, NTNU.

Wilthil, E.F., Flåten, A.L., and Brekke, E.F. (2017). A target tracking system for ASV collision avoidance based on the PDAF. In *Sensing and Control for Autonomous Vehicles*, 269–288. Springer.